Chemical Physics Letters 518 (2011) 38–43

Contents lists available at SciVerse ScienceDirect

Chemical Physics Letters

journal homepage: www.elsevier.com/locate/cplett

Vacuum ultraviolet mass-analyzed threshold ionization spectroscopy of methylcyclohexane in the supersonic jet

Songhee Han [a], Hyun Sik Yoo [a], Doo-Sik Ahn [a], Young S. Choi [b,*], Sang Kyu Kim [a,*]

[a] Department of Chemistry and KI for Nanocentury, KAIST, Daejeon 305-701, Republic of Korea
[b] Department of Chemistry, Inha University, Incheon 402-751, Republic of Korea

ARTICLE INFO

Article history:
Received 9 September 2011
In final form 1 November 2011
Available online 7 November 2011

ABSTRACT

Vacuum ultraviolet (VUV) mass-analyzed threshold ionization (MATI) spectrum of supersonically cooled methylcyclohexane has been obtained to give the precise adiabatic ionization energy of 9.6958 ± 0.0025 eV for the chair equatorial conformer. Vibrationally resolved MATI spectrum has been analyzed with the aid of density functional theory and Franck–Condon calculations. The MATI spectrum reflects the structural change upon ionization and its origin is discussed by inspecting the shapes of the valence orbitals involved in the ionization process. The spectroscopic implication of the structural interconversion above the certain energy level is discussed with theoretical calculations of molecular structures and energetics.

1. Introduction

Cyclohexane molecules have been intensively studied as a prototypical model system for the conformational chemistry, and a substantial experimental and theoretical effort has been given to understand conformational interconversion processes of these floppy molecules at the molecular level [1–6]. Mono-substituted cyclohexane molecules have been particularly spotlighted as the energetics and dynamics of their equatorial and axial conformers may provide keys for the origin of anomeric and/or steric effects as well as conformer-specific reactivity [7–14]. Methylcyclohexane belongs to this case. In previous other studies, it has been found that the equatorial conformer is more stable than the axial conformer for methylcyclohexane, as revealed by NMR [15], electron diffraction [16,17], or thermochemical studies [18]. The conformational preference of methylcyclohexane had also been confirmed by theoretical calculations [10]. However, the ionization of the title molecule, even though it may provide essential information about the role of the valence orbital in the chemical reactivity or thermodynamic stability, has been little studied to date [19–23].

Mass-analyzed threshold ionization (MATI) or zero-electron kinetic energy (ZEKE) spectroscopic technique combined with the supersonic jet method has been widely used in many laboratories since it provides the excellent energy resolution with a relatively simple pulsed-field ionization scheme [24]. One-photon MATI spectroscopy using the vacuum ultraviolet (VUV) laser source is particularly useful for molecular systems with no stable ladder in the two-color ionization process, and has been employed for the ionization of various biological building blocks [25–27] or molecular structural isomers [28,29] to reveal the role of the valence electron in the molecular structure and associated chemical reactivity. Here, photoionization of methylcyclohexane has been investigated using the VUV–MATI technique, providing the precise ionization energy of the equatorial methylcyclohexane conformer and vibrational frequencies of the cationic ground state. With the aid of density functional theory (DFT) calculations, activated vibrational modes in the MATI spectrum have been appropriately assigned. The structural change upon ionization and conformational interconversion in the cationic ground state are discussed with theoretical calculations.

2. Experiment

The detailed experimental setup had been reported in our previous report [30]. Briefly, methylcyclohexane (Aldrich, anhydrous 99 + %) was heated to 50 °C, seeded in Ar, and expanded into a vacuum chamber through a nozzle orifice (General valve, 0.5 mm diameter) with a backing pressure of 1 atm. The supersonic jet of molecular beam was collimated through a 1 mm diameter skimmer (Precision) before it was collinearly overlapped with the VUV laser pulse. The background pressure of 10^{-7} Torr was maintained when the nozzle was operated with a repetition rate of 10 Hz. The VUV laser pulse was generated via four-wave mixing in a Kr gas cell by combining the UV laser pulse fixed at 212.556 nm for the Kr $5p[1/2]_0$-$4p^6$ transition and a tunable VIS laser pulse in the 625–684 nm range. Then, the VUV pulse was spatially separated from UV and VIS fundamentals using the edge of the calcium fluoride (CaF_2) collimating lens placed at the exit of the Kr cell where the pressure was maintained at 1 Torr. The wavelength of VIS laser pulse was calibrated with a wavemeter (Coherent; Wavemaster). High-*n*,*l*

* Corresponding authors.
E-mail addresses: yschoi@inha.ac.kr (Y.S. Choi), sangkyukim@kaist.ac.kr (S.K. Kim).

0009-2614/$ - see front matter © 2011 Elsevier B.V. All rights reserved.
doi:10.1016/j.cplett.2011.11.005

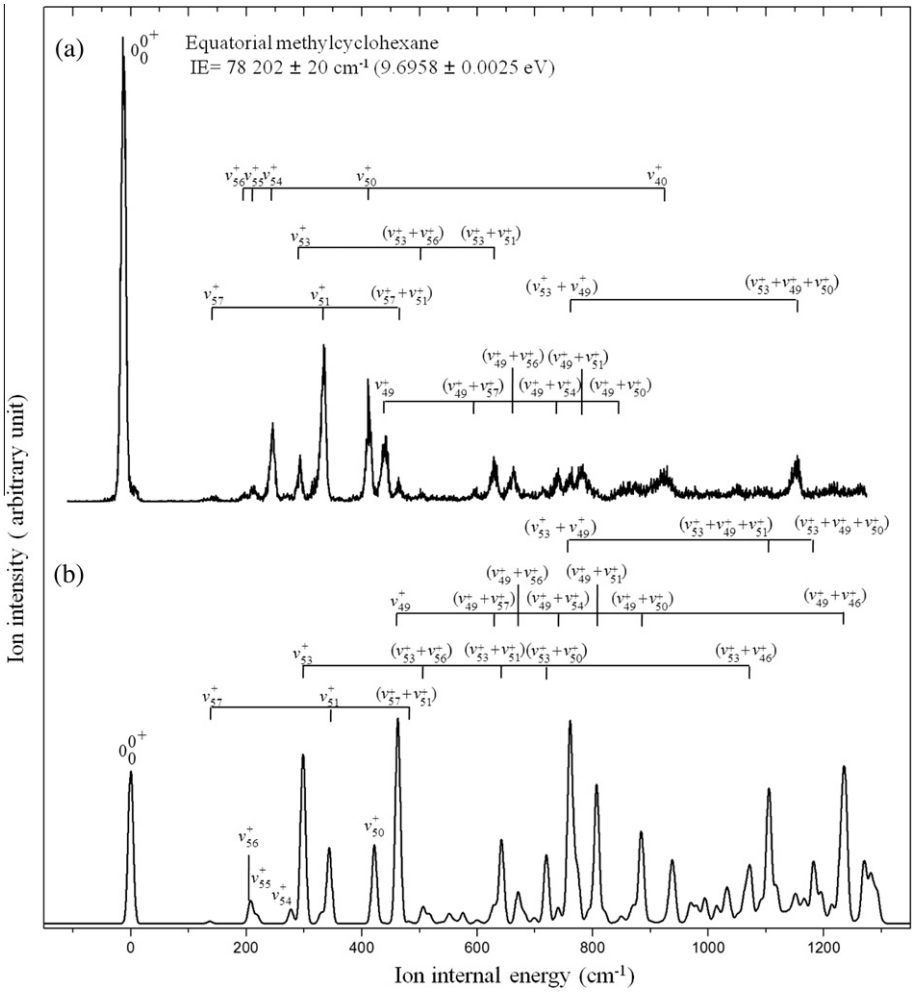

Figure 1. (a) The VUV–MATI spectrum of methylcyclohexane with (b) Franck–Condon simulation spectrum based on the B3LYP/6-311++G(d,p) calculations for the equatorial conformer. The combination bands are represented in the parentheses. See Table 2 for the description of normal modes given by numbers.

Table 1
Relative stabilization energies (cm^{-1}) of the optimized equatorial and axial conformers of methylcyclohexane in the neutral (S_0) and cationic (D_0) ground states obtained from B3LYP/6-311++G(d,p) calculations. Zero-point energy corrected values are given in parentheses.

Conformer (point group)	B3LYP/6-311++G(d,p)	
	S_0	D_0
Equatorial (C_1)	0 (21.73)	0 (0)
Equatorial (C_S)	4.39 (0)	1058.92 (813.81)[a]
Axial (C_S)	762.57 (814.03)	1385.33 (896.99)

[a] This value is for the transition state structure.

Rydberg states of molecules which were generated by the excitation with VUV laser pulse were pulsed-field ionized (~10 V/cm) at the delay time of ~20 μs after the laser pulse excitation, which is long enough for the complete separation of the MATI signal from prompt ion signals along the time-of-flight tube. Thus no spoil field was necessary in this scheme. Pulsed-field ionized species were repelled, accelerated, drifted along the time-of-flight axis, and detected by dual microchannel plates (MCP). Ion signals were digitized by an oscilloscope (LeCroy, LT584M) and stored in a personal computer that controlled all step motors to scan laser wavelengths for the molecule excitation.

3. Computational details

All calculations were carried out using the Gaussian 03W program package [31]. The minimum energy structures and normal modes for ground neutral and cationic states were obtained with the B3LYP/6-11++G(d,p) level of calculation [32,33]. The intrinsic reaction coordinate (IRC) calculation for the cationic state was performed at the same level, starting from the transition state with the force constant calculations at each point. The Franck–Condon analysis was done using the Duschinsky transformation [34] with a code developed by Peluso and coworkers [35,36].

Table 2
Some of experimental and calculated vibrational frequencies (cm^{-1}) of the equatorial conformer of methylcyclohexane in the cationic (D_0) ground states obtained at the B3LYP/6-311++G(d,p) level of calculation.

	Equatorial		
	D_0		Description[a]
	Calc.	Expt.	
ν_{57}^+	137	147	Ring puckering
ν_{56}^+	208	198	$C_{(7)}H_3$ rock
ν_{55}^+	219	213	Asym. $C_{(2,3,5,6)}H_2$ wag
ν_{54}^+	277	246	$C_{(1)}$-$C_{(7)}H_3$ distortion
ν_{53}^+	298	293	Ring bend
ν_{52}^+	330		Asym. $C_{(3,4,5)}H_2$ wag
ν_{51}^+	344	335[c]	$C_{(1)}$-$C_{(7)}H_3$ distortion
ν_{50}^+	422	411[c]	$C_{(6)}C_{(1)}C_{(7)}$ bend
ν_{49}^+	463	441	Ring distortion
	481[b]	464	$\nu_{57}^+ + \nu_{51}^+$
	491[b]	505	$\nu_{56}^+ + \nu_{53}^+$
ν_{48}^+	519		Sym. $C_{(3,4,5)}H_2$ wag
	588[b]	598	$\nu_{57}^+ + \nu_{49}^+$
	628[b]	628	$\nu_{53}^+ + \nu_{51}^+$
	639[b]	663	$\nu_{56}^+ + \nu_{49}^+$
	687[b]	718	$\nu_{54}^+ + \nu_{49}^+$
ν_{47}^+	729		Sym. $C_{(2,3)}H_2$ wag
	734[b]	764	$\nu_{53}^+ + \nu_{49}^+$
	776[b]	783	$\nu_{51}^+ + \nu_{49}^+$
ν_{46}^+	774		$C_{(6)}H_2$ wag
ν_{45}^+	808		Sym. $C_{(3,5)}H$ wag
ν_{44}^+	821		Asym. $C_{(2,3,5,6)}H_2$ wag
	852[b]	835∼874∼884[d]	$\nu_{50}^+ + \nu_{49}^+$
ν_{43}^+	868		$C_{(3,4,5)}H$ wag
ν_{42}^+	872		$C_{(4)}H_2$ wag
ν_{41}^+	891		$C_{(7)}H_2$ rock
ν_{40}^+	937	922	Asym. $C_{(1,2)}H$ rock
ν_{39}^+	941		$C_{(2,6,7)}H_2$ wag
ν_{38}^+	982		$C_{(1,2,5,6)}H_2$ rock
ν_{37}^+	994		$C_{(4)}H_2$ rock
ν_{36}^+	1032		Asym. $C_{(1,2,3,5,6,7)}H$ wag
ν_{35}^+	1038		Sym. $C_{(3,6)}H$ rock
	1069[b]	1050	$\nu_{53}^+ + \nu_{51}^+ + \nu_{49}^+$
ν_{34}^+	1054		Asym. $C_{(5,6)}H$ wag
ν_{33}^+	1092		$C_{(1)}$-$C_{(7)}H_3$ str.
ν_{32}^+	1129		Asym. $C_{(4,5,6)}H$ wag
ν_{31}^+	1188		$C_{(1)}H$ rock
ν_{30}^+	1213		$C_{(2)}H_2$ wag
ν_{29}^+	1228		Asym. $C_{(2,5)}H_2$ wag
ν_{28}^+	1245		Asym. $C_{(2,4)}H_2$ wag

[a] Refer Table 3 for the atomic labeling.
[b] Calculated based on the experimental values of fundamental modes.
[c] The most activated vibrational modes in the MATI spectrum.
[d] The broad energy range appeared in the MATI spectrum.

4. Results and discussion

Whereas methylcyclohexane exists as one predominant stable configuration of the chair form, the methyl group may adopt either axial or equatorial position of the cyclohexane-like skeletal structure. The energy difference of axial and equatorial conformers of the chair methylcyclohexane molecule had been estimated to be 1.75 ± 0.05 kcal/mol (612 cm^{-1}) in solution [15] or 1.9–2.0 kcal/mol (665–670 cm^{-1}) in the gas phase. Accordingly, the relative abundance of the equatorial conformer is estimated to be 96% at 19 °C in the gas phase [18], and thus the equatorial conformer may be dominant in the molecular beam. The strongly observed peak at 78 202 cm^{-1} in the VUV–MATI spectrum in Figure 1a, therefore, should correspond to the adiabatic ionization energy of the chair equatorial methylcyclohexane, giving IE = 9.6958 ± 0.0025 eV. This value is most precise one to date as compared to previously reported values. Our DFT calculations at the B3LYP/6-311++G(d,p) level also predict that the equatorial conformer is more stable both in neutral and cationic ground states (Table 1).

A number of vibrational bands of the cationic ground state have been identified in the VUV–MATI spectrum, Figure 1. Low-frequency vibrational bands with the energy less than 450 cm^{-1} are quite active in the MATI spectrum, and these are appropriately assigned based on the comparison with the theoretical prediction as described in Table 2. The ν_{54}^+ mode assignment is rather tentative as the experiment is off by ∼30 cm^{-1} from the theoretical value. This discrepancy though is not surprising for the low-frequency vibrational mode of the floppy molecule such as methylcyclohexane, especially because the corresponding mode involves the entire molecular skeletal distortion. The MATI band at 335 cm^{-1} is particularly intense, and this may be due to the ν_{51}^+ mode, corresponding to the $C_{(1)}$–$C_{(7)}H_3$ distortion, Figure 2. Combination bands associated with the ν_{51}^+ band are found to be quite active, Figure 1 and Table 2. The next strongest band at 411 cm^{-1} is assigned to ν_{50}^+,

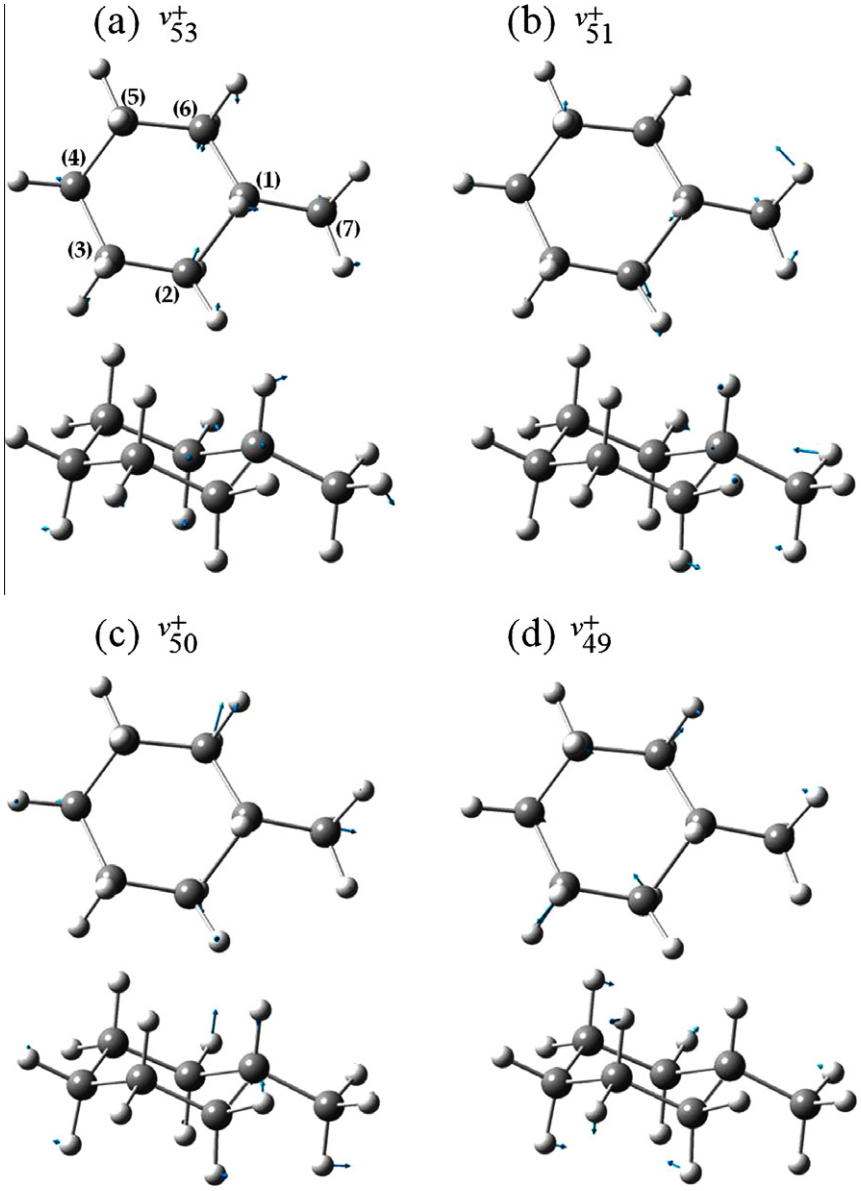

Figure 2. Vector representations of (a) v_{53}^+, (b) v_{51}^+, (c) v_{50}^+ and (d) v_{49}^+ vibrational modes of the equatorial methylcyclohexane calculated by B3LYP/6-311++G(d,p). The upper represents the top view while the bottom is the side view.

corresponding to $C_{(6)}C_{(1)}C_{(7)}$ bend, and its combination bands are quite evident in Figure 1 and Table 2. The bands at 293 and 441 cm^{-1} are ascribed to v_{53}^+ ring bend and v_{49}^+ ring distortion modes, respectively. These spectroscopic characteristics of the VUV–MATI spectrum reflect the structural change of the molecule upon ionization. Our B3LYP/6-311++G(d,p) calculations (Table 3) show that bond length of $R(C_{(1)}–C_{(2)})$ and angles of $\angle C_{(2)}C_{(1)}C_{(7)}$,$\angle C_{(6)}C_{(1)}C_{(7)}$,$\angle HC_{(1)}C_{(7)}$ and $\angle C_{(2)}C_{(1)}C_{(6)}$ change quite significantly as the molecule is being ionized, and it explains why the v_{51}^+ and v_{50}^+ modes are activated in the MATI spectrum. The origin of the structural change upon ionization can be found from the inspection of the molecular orbtials before and after the ionization. For methylcyclohexane, electron density of the highest-occupied molecular orbital (HOMO) is found to be quite delocalized over the entire molecule, Figure 3. The removal of an electron from HOMO upon ionization gives the unpaired electron residing in the singly-occupied molecular orbital (SOMO). The electron density of SOMO is also calculated to be almost evenly distributed whereas the position of orbital node is quite asymmetric compared to that of HOMO about the C_S plane bisecting the angles of $\angle C_{(3)}C_{(4)}C_{(5)}$ and $\angle C_{(2)}C_{(1)}C_{(6)}$. This small but critical difference in the orbital shape of HOMO and SOMO seems to be responsible for the activation of v_{51}^+ and v_{50}^+ modes in which the nuclear displacements of the methyl moiety are quite dominant. Other low-frequency ring skeletal modes in MATI seem to be also explainable by this orbital shape difference.

Our DFT calculation predicts that the neutral ground methylcyclohexane adopts the C_S geometry at the minimum energy. The C_1 geometry in the ground state is only slightly different from the C_S geometry with a small energy difference of 22 cm^{-1} (Tables 1 and 3). On the other hand, the C_1 and C_S geometries become quite distinct upon ionization. The C_1 geometry is calculated to be more stable than the C_S geometry by 814 cm^{-1} in the cationic ground state. The Franck–Condon simulated spectrum assuming C_1 geometries for both neutral and cationic ground states describes band intensities of the MATI spectrum rather poorly, particularly at the high internal energy region, Figure 1. It is found that only weak and broad bands are observed at the energy region higher than ~800 cm^{-1} above the ionization threshold in the MATI spectrum,

Table 3
The C_1 geometrical parameters (Å, °) of the neutral and cationic ground states of the equatorial methylcyclohexane calculated at the B3LYP/6-311++G(d,p) level.

	Equatorial(C_1)		
	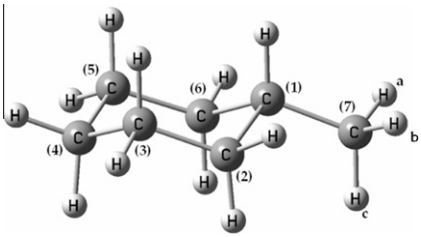		
	S_0	D_0	Diff[a]
$R(C_{(1)}–C_{(7)}H_3)$	1.53	1.50	−2.10
$R(C_{(1)}–C_{(2)})$	1.54	1.81	17.76
$R(C_{(2)}–C_{(3)})$	1.54	1.49	−3.23
$R(C_{(3)}–C_{(4)})$	1.53	1.52	−0.74
$R(C_{(4)}–C_{(5)})$	1.54	1.56	1.30
$R(C_{(5)}–C_{(6)})$	1.54	1.52	−0.96
$R(C_{(6)}–C_{(1)})$	1.54	1.50	−2.36
$\angle C_{(2)}C_{(1)}C_{(7)}$	111.68	105.34	−5.68
$\angle C_{(6)}C_{(1)}C_{(7)}$	111.74	118.83	6.34
$\angle HC_{(1)}C_{(7)}$	107.95	113.37	5.02
$\angle C_{(2)}C_{(1)}C_{(6)}$	110.31	103.01	−6.61
$\angle C_{(3)}C_{(4)}C_{(5)}$	111.34	108.43	−2.62
$\angle C_{(1)}C_{(2)}C_{(3)}$	112.32	106.95	−4.78
$\angle C_{(1)}C_{(6)}C_{(5)}$	112.37	116.29	3.49
$\angle C_{(2)}C_{(3)}C_{(4)}$	111.60	115.31	3.33
$\angle C_{(4)}C_{(5)}C_{(6)}$	111.55	110.02	−1.37
$\angle C_{(3)}C_{(2)}C_{(1)}C_{(7)}$	−179.10	−179.22	0.07
$\angle C_{(5)}C_{(6)}C_{(1)}C_{(7)}$	179.07	174.11	−2.77

[a] Difference between geometrical parameters of neutral and cation, which is based on the equation of (neutral-cation)/neutral × 100.

whereas a number of strong vibrational bands are predicted to be persistent in the simulation. This rather sharp decrease of the band intensity in MATI suggests that the internal energy excitation may induce the conformational change in the cationic ground state. Actually, the calculated energy difference of 814 cm^{-1} between C_1 and C_S geometries of the cationic ground state is close to the ion internal energy where the MATI band intensity starts to decrease quite sharply.

The experimental fact that the most active MATI bands of ν_{51}^{+} or ν_{50}^{+} are associated with the asymmetric swing motion of the methyl group strongly supports that the $C_S \rightarrow C_1$ geometrical transition occurs in the one-photon excitation from the neutral to the cationic ground state. Naturally, above the barrier of the interconversion between two equivalent C_1 geometries, the density of states increases, and the Franck–Condon factors should be distributed over many quantum states, resulting in the decrease of the spectral intensity. Intrinsic reaction coordinate (IRC) calculation confirms this structural change and associated reaction coordinate, Figure 4. A smooth energetic diagram is obtained as a function of the dihedral angle between the plane of $C_{(5)}C_{(6)}C_{(1)}$ atoms and that of $C_{(6)}C_{(1)}C_{(7)}$, respectively.

5. Summary

In summary, vacuum ultraviolet (VUV) mass-analyzed threshold ionization (MATI) spectroscopy has been carried out to provide the most accurate and precise adiabatic ionization energy of 9.6958 ± 0.0025 eV for the equatorial conformer of the chair methylcyclohexane. Vibrational structures revealed in the MATI spectrum are analyzed using DFT calculations at the B3LYP/6-311++G(d,p) level. The electron deficiency in the highest-occupied molecular orbital (HOMO) and the significant change of the orbital shape in the singly-occupied molecular orbital (SOMO) in terms of the orbital node position explain the structural change upon ionization quite well at least qualitatively. Our calculations suggest that the minimum energy structure of the cationic ground state adopts the C_1 geometry and two equivalent C_1 structures interconvert through the C_S transition state with a barrier of 814 cm^{-1}. The MATI spectrum showing a rather sharp decrease of the ion signal at ~800 cm^{-1} of the ion internal energy may indicate that the conformational interconversion really occurs in the cationic ground state. One-photon MATI spectrum of the floppy methylcyclohexane molecule turns out to be very useful not only in terms of the static information such as

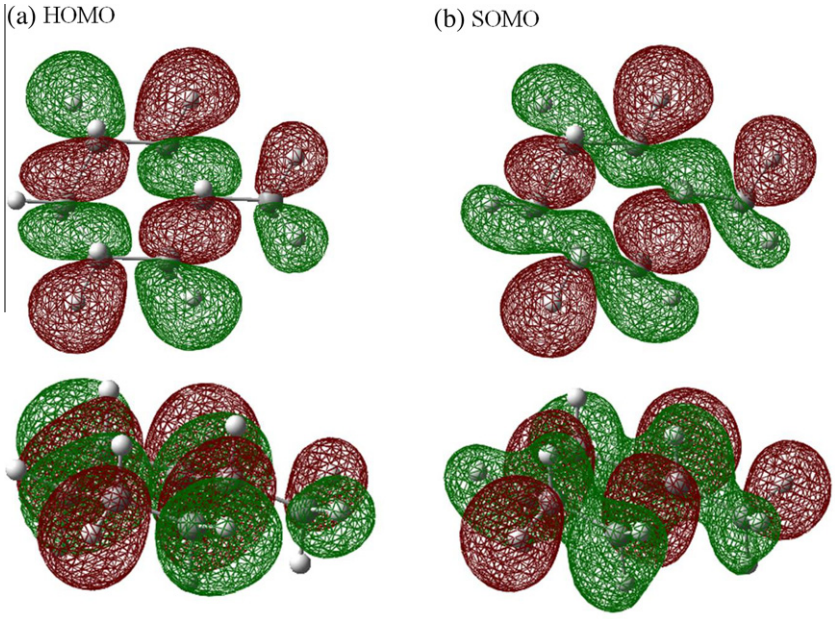

Figure 3. (a) Highest-occupied molecular orbital (HOMO) and (b) singly-occupied molecular orbital (SOMO) of the equatorial methylcyclohexane conformer obtained from B3LYP/6-311++G(d,p) calculations. Top and bottom views are drawn in the upper and lower parts, respectively.

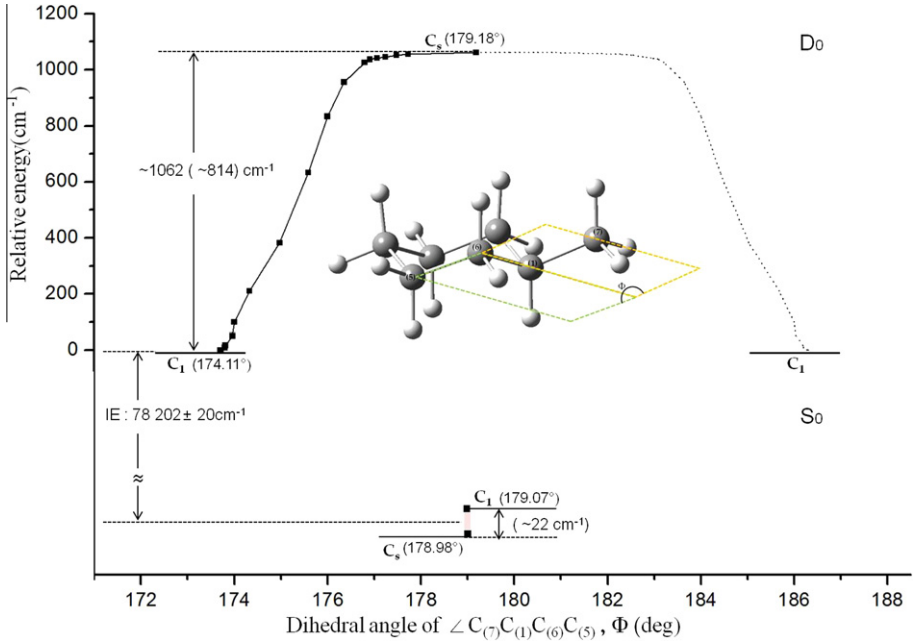

Figure 4. Schematic curve connecting the C_1 and C_S symmetry structures of the equatorial methylcyclohexane in the cationic ground state (D_0) using IRC calculation as a function of the conformational coordinate (square dots). The values in parentheses represent $\angle C_{(7)}C_{(1)}C_{(6)}C_{(5)}$ dihedral angles for the C_1 or C_S structures in Table 3. The shaded region represents the dihedral angles of the C_1 or C_S symmetry minimum energy structures in the neutral ground state (S_0). Zero point energy corrected value of the barrier height for the structural interconversion in the D_0 state is ~814 cm^{-1}, and the one corresponding to the energy difference between C_1 and C_S symmetry structures in S_0 state is ~22 cm^{-1},Table 1. The experimental value of IE is from this work.

ionization energy and cationic vibrational frequencies but also in terms of dynamic information such as the conformational isomerism.

Acknowledgement

This work was supported by the National Research Foundation of Korea (NRF) grant funded by the Korea government (MEST; 2011-0001216, 2011-0016447). S. Han was supported by the project of National Junior research fellowship which National Research Foundation of Korea conducts from 2010 (2011-0001762).

References

[1] H.L. Strauss, H.M. Pickett, J. Am. Chem. Soc. 92 (1970) 7281.
[2] R.A. Kuharski, D. Chandler, J.A. Montgomery, F. Rabii, S.J. Singer, J. Phys. Chem. 92 (1988) 3261.
[3] M.A. Wilson, D. Chandler, Chem. Phys. 149 (1990) 11.
[4] B. Sirjean, P.A. Glaude, M.F. Ruiz-Lopez, R. Fournet, J. Phys. Chem. A 110 (2006) 12693.
[5] K. Kakhiani, U. Lourderaj, W.F. Hu, D. Birney, W.L. Hase, J. Phys. Chem. A 113 (2009) 4570.
[6] S. Holly, G. Jalsovszky, O. Egyed, J. Mol. Struct. 79 (1982) 465.
[7] L. Pierce, J.F. Beecher, J. Am. Chem. Soc. 88 (1966) 5406.
[8] F.R. Jensen, C.H. Bushweller, B.H. Beck, J. Am. Chem. Soc. 91 (1969) 344.
[9] D. Damiani, L. Ferretti, Chem. Phys. Lett. 21 (1973) 592.
[10] M.d.C. Fernández-Alonso, J. Cañada, J. Jiménez-Barbero, G. Cuevas, Chem. Phys. Chem. 6 (2005) 671–680.
[11] Q. Shen, J.M. Peloquin, Acta Chem. Scand. A 42 (1988) 367.
[12] E.L. Eliel, R.J.L. Martin, J. Am. Chem. Soc. 90 (1968) 682.
[13] L.W. Reeves, K.O. Stromme, Can. J. Phys. 38 (1960) 1241.
[14] S. Han, H.S. Yoo, S.K. Kim, J. Phys. Chem. A 114 (2010) 10005.
[15] H. Booth, J.R. Everett, J. Chem, Soc. Perkin Trans. 2 (1980) 255.
[16] A. Tsuboyama, A. Murayama, S. Konaka, M. Kimura, J. Mol. Struct. 118 (1984) 351.
[17] H.J. Geise, H.R. Buys, F.C. Mijlhoff, J. Mol. Struct. 9 (1971) 447.
[18] C.W. Beckett, K.S. Pitzer, R. Spitzer, J. Am. Chem. Soc. 69 (1947) 2488.
[19] K. Watanabe, T. Nakayama, J. Mottl, J. Quant. Spectry. Radiative Transfer 2 (1962) 369.
[20] S. Rang, P. Paldoia, A. Talvari, Eesti. NSV Tead. Akad. Toim. (1974) 354.
[21] M. Meot-Ner, L.W. Sieck, P. Ausloos, J. Am. Chem. Soc. 103 (1981) 5342.
[22] L.W. Sieck, M. Mautner, J. Phys. Chem. 86 (1982) 3646.
[23] J.L. Holmes, F.P. Lossing, Org. Mass Spectrom. 26 (1991) 537.
[24] K. Muller-Dethlefs, E.W. Schlag, Annu. Rev. Phys. Chem. 42 (1991) 109.
[25] K.-W. Choi, J.-H. Lee, S.K. Kim, J. Am. Chem. Soc. 127 (2005) 15674.
[26] K.-W. Choi, J.-H. Lee, S.K. Kim, Chem. Commun. (2006) 78–79.
[27] S. Han, T.Y. Kang, S. Choi, K.-W. Choi, S.J. Baek, S. Lee, S.K. Kim, Phys. Chem. Chem. Phys. 10 (2008) 3883.
[28] S. Choi, Chem. A 112 (2008) 5060.
[29] S. Choi, Chem. A 112 (2008) 7191.
[30] K.-W. Choi, S. Choi, S.J. Baek, S.K. Kim, J. Chem. Phys. 126 (2007). 034308–034308.
[31] M.J.T. Frisch et al., Gaussian Inc., Wallingford, CT, 2004.
[32] A.D. Becke, J. Chem. Phys. 98 (1993) 5648.
[33] A.D. Becke, Phys. Rev. A 38 (1988) 3098.
[34] F. Duschinsky, Acta Physicochim. USSR 7 (1937) 551.
[35] A. Peluso, F. Santoro, G.D. Re, Int. J. Quantum. Chem. 63 (1997) 233.
[36] R. Borrelli, A. Peluso, J. Chem. Phys 119 (2003) 8437.